2006-01-0460

Effect of Active Muscle Forces on the Response of knee Joint at Low Speed Lateral Impacts

Anurag Soni, Anoop Chawla and Sudipto Mukherjee
Indian Institute of Technology Delhi, Department of Mechanical Engineering, India

ABSTRACT

In vehicle-pedestrian collisions, lower extremities of pedestrians are frequently impacted by the vehicle front structure. The aim of the current study is to understand the role of muscle activity in knee joint injuries at low velocity lateral impacts, characteristic of vehicle-pedestrian collisions. Therefore, a group of muscles in the lower extremity are modeled using bar elements with the Hill material model. The reflex response of the muscle is then included. Simulations indicate that muscle activation decreases the probability of failure in knee ligaments.

INTRODUCTION

The issue of pedestrian safety has been a matter of concern for public health practitioners and vehicle designers (Ashton et al., 1977). Pedestrians represent 65% of the 1.17 million people killed annually in road accidents worldwide (World Bank, 2001). Epidemiological studies on pedestrian victims have indicated that together with the head, the lower extremities are the most frequently injured body region (Chidester et al., 2001; Mizuno, 2003). The 2003 summary report of International Harmonized Research Activities (IHRA) Pedestrian Safety Working Group activity (Mizuno, 2003) has showed that 1,605 pedestrian victims in Australia, Germany, Japan and USA, sustained a total of 3,305 AIS 2+ injuries, out of which almost one third (32.6%) were to the lower extremity. The injuries to lower extremities in car crashes mainly include bone fractures and avulsion or stretching in knee ligaments (Mizuno, 2005). To mitigate the incidences and extent of lower limb injuries, it is essential to understand the mechanism of these injuries, and both experimental as well as numerical methods have been widely used for this purpose.

For ethical reasons, volunteer experiments cannot be performed in the higher injury severity range similar to those in pedestrian-car crashes. Therefore, the loading environment in pedestrian-car collisions has been characterized by experiments using Post Mortem Human Specimens (PMHS) (Bunketorp et al., 1981; 1983; Aldman et al., 1985; Kajzer et al., 1990; 1993; 1997; 1999; Ramet et al., 1995; Bhalla et al., 2003; 2005; Kerrigan et al., 2003; Bose et al., 2004; Ivarsson et al., 2004; 2005). As cadavers have been used in these experiments, these studies could not consider the effect of live muscle actions such as involuntary muscle reflexes, pre-impact voluntary muscle bracing etc. Mechanical legforms (the EEVC legform by TRL; FlexPLI (Konosu et al., 2005); Polar II pedestrian dummy by Honda R&D; frangible legform by Dunmore et al., 2005) have also been developed on the basis of these tests, and as a result do not account for muscle forces. Finite element (FE) studies offer an alternate method of studying these effects.

Based on the results of PMHS studies, validated FE models of pedestrian lower extremities have been developed, and the knee injury mechanism and criteria have been investigated (Schuster et al., 2000; Maeno et al., 2001; Takahashi et al., 2001; 2003; Matsui et al., 2001; Nagasaka et al., 2003; Chawla et al., 2004). However, these FE models have not included the effect of muscle actions, as yet.

Thus, neither the human surrogates nor the current FE models include the effect of live muscles. It is however reported that muscle active forces reduce the risk of injuries in soft tissues (Brolin et al., 2005). According to Pedestrian Crash Data Studies (PCDS) (Chidester et al., 2001), pedestrian accidents occur for various pre-impact postures. Postures are maintained due to muscle forces. Louie et al., (1984) asserted that effective stiffness of the knee joint increases with increase in muscle activation and the number of recruited muscles. Pope et al., (1979) have also demonstrated that muscles contracted for posture control or for other motion function affect the loading at the knee joint. Therefore, muscle forces are expected to affect stresses and injuries in crashes.

To verify the hypothesis that contracted muscles protect the knee joint during rapid loading, we have investigated the effects of pre-impact active muscle forces on knee ligament forces in pedestrian accidents using finite element models. We have added muscles in the lower extremity model of the THUMS human body model that was validated for passive response by Chawla et al., (2004). The muscle elements, represented as bar

elements, were assigned the Hill material model to simulate the effect of muscular contraction.

In order to study the effect of muscles, we have chosen the leg configuration used by Kajzer et al., (1997; 1999). The results obtained with deactivated muscles have been compared with Kajzer experimental results as well as simulation results from Chawla et al., (2004). Our choice of this configuration was based on availability of the base model and experimental data. The PCDS study (Chidester et al., 2001) reports that this configuration is a low probability event (only a 5% likelihood of occurrence in pedestrian accidents). However, we have opted for this configuration because our study focuses on change caused by inclusion of muscle activation and is not targeted at quantifying injuries in real crash situations, as yet. Konosu et al., 2005 have raised issues about the fidelity of the boundary conditions used in Kajzer tests and the accuracy of their bending moment calculations. However, in this study, we needed a validated FE model that has the overall characteristics exhibited by the human knee. Issues about the relevance of boundary conditions and the accuracy of bending moment calculations are hence not important in this study.

After validating our model and the muscle definitions, we have modeled a pedestrian in a standing posture with muscle activation. Only the muscle forces required to maintain the standing human posture are modeled (without any evasive action) in the pre-impact stage. Stretch reflex, by which an automatic counteraction stabilizes a muscle to over stretching, was also modeled in simulation. Ligament forces with and without muscle activation for this posture have then been compared.

MATERIALS AND METHODS

FINITE ELEMENT MODEL DESCRIPTION

In the present work, the lower extremity model validated by Chawla et al., (2004) was used as a base model and 40 lower extremity muscles were modeled on it using 1-D bar elements.

Figure 1 shows the FE mesh of the simulation set up. The model included the cortical and the spongy parts of the pelvis, the femur, tibia, fibula, and the patella. The cortical part of the bones was modeled by shell elements while the spongy part was modeled by solid elements. Apart from these, passive muscle and skin were also modeled using solid elements and membrane elements respectively. The four major knee ligaments, the anterior cruciate ligament (ACL), the posterior cruciate ligament (PCL), medial collateral ligament (MCL) and the lateral collateral ligament (LCL), were modeled using membrane elements. The default material properties defined in THUMS have been retained in this study.

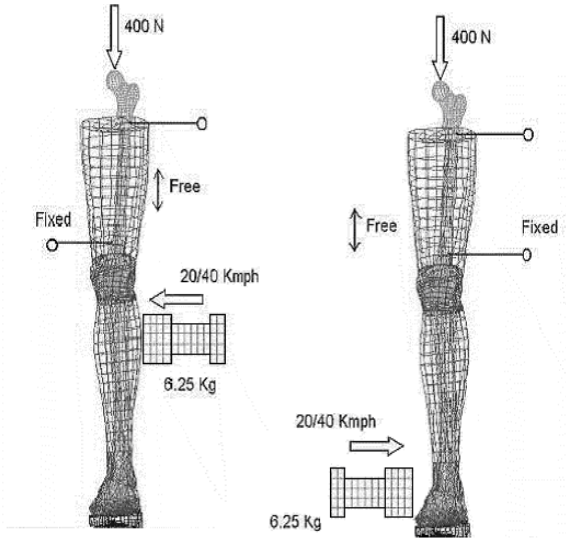

Figure 1 Modified THUMS model validated by Chawla et al., 2004 for shear and bending load conditions of Kajzer test

MUSCLE MODELING

Mathematical models of lower extremity muscles have been widely used to predict muscle and joint forces in gait studies (Dul et al., 1984a; 1984b; Seireg et al., 1973; Yeo, 1976; Hardt et al., 1978; Pedotti et al., 1978; Crowninshield et al., 1981; Davy et al., 1987; White et al., 1989; Glitch et al., 1997). Of late, Brolin et al., (2005) has incorporated neck muscles in a finite element model of the human cervical spine to study neck response in traffic accidents. He showed that muscle activation decreases the risk of injury to spinal ligaments. An accurate representation of muscle geometric parameters such as moment arm, fiber pennation angle, muscle fiber length, and muscle size is needed to accurately model the muscles.

Muscles follow curved paths due to the presence of bony prominences and other soft tissues. The exact way of representing a muscle's line of action about a joint would be to describe its three-dimensional centroidal path on bones. However, the detailed description of a muscle's centroidal path is complex. Therefore muscles are assumed to act along straight lines from origin to insertion (Brand et al., 1982).

Investigators have used a variety of methods to identify the origin of the lower extremity muscles and the location of the point of insertion on the bone segment. Brand et al., (1982); Friedrich and Brand, (1990); Seireg and Arvikar, (1989) and Wickiewicz et al., (1983) have dissected the fresh and embalmed cadavers, whereas Pierrynowski and Morrison, (1985); Dostal and Andrews, (1981); White et al., (1989); have identified the center of muscle attachment points by measuring relevant points on polymer models of bones. Yamaguchi et al., (1990) report an extensive survey of human musculoskeletal actuator parameters, including data from many published sources. Subsequently Kepple et al., (1998) generated an extensive three-dimensional database of

lower extremity musculoskeletal system from 52 dried skeletal specimens.

In the present study, we have used the data of origin and insertion locations of the muscles as reported in White et al., (1989). The basis for selection of this specific database was the similarity in height of the reported male specimen (177 cm) and the THUMS model (175 cm).

The points of origin and the orientations of four local reference frames at the pelvic, femur, tibia and foot, defined by White et al., (1989), were reproduced using Altair Hyper Mesh™. Origin and insertion locations of each muscle were then digitized and mapped on to the FE mesh of the cortical bone segments. The nodes nearest to the two identified locations were selected and joined by 1-D bar element to represent a muscle. Figure 2 shows the lower extremity muscles thus modeled. According to Brand et al., (1982), some muscles with broad origin (e.g. Glutes Maximus, Glutes Medius, Glutes minimus) or broad insertions (e.g. Glutes Maximus, adductor brevis, adductor magnus) should be defined by multiple bar elements to account for functional independence in the different groups of muscle fibers and their effect on torque prediction. However, certain muscles like Vastus Internmedius and Soleus have a broad origin and insertion, but can be defined by single bar elements without significantly affecting torque prediction (Brand et al., (1982))

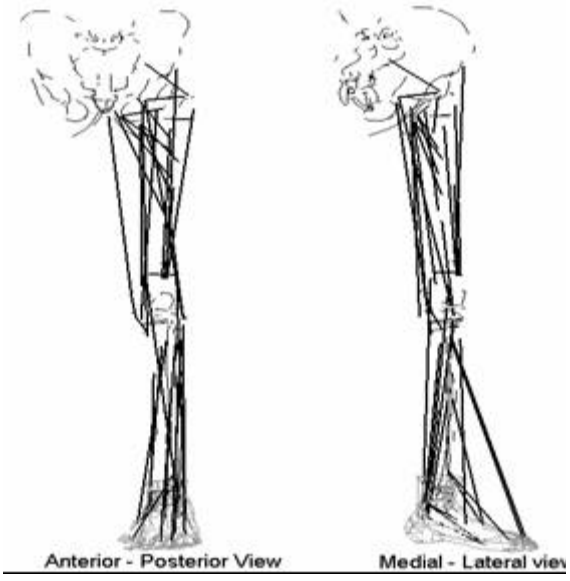

Figure 2. Anterior-posterior and Medial-Lateral views showing 40 lower extremity muscles modeled as bar elements for a standing posture. Origin and insertion location of these muscles are defined according to White et al. (1989).

Muscle parameters, such as optimal muscle length (L_{opt}), maximum isometric force (F_{max}), maximum contraction/ elongation velocity (V_{max}), pennation angle (α), and an initial value of activation level (N_a), are required to define the Hill type muscle bar element. The initial activation level (N_a) is defined as the ratio of a current force to the maximum force that can be exerted by a muscle. Thus it is a dimensionless quantity whose range is set in Pamcrash™ to have a minimum value of 0.005 to maximum value of 1. Activation value of 0.005 represents a muscle at rest whereas maximum value (i.e.1) represents maximum activation in a muscle, such as that for a maximum voluntary contraction (Winters et al., 1988). Optimal muscle length and maximum velocity of a muscle are related to the muscle fiber length at rest (L_{ofib}). The muscle length at rest was taken to be the distance between the nodes where the muscle element terminates. Maximum isometric force was calculated from Physiological Cross-Section Area (PCSA) and maximum muscle stress. The maximum muscle stress varies from 20 N/cm^2 to 100 N/cm^2 (Winters et al., 1988). Brolin et al., (2005) has reported a value of 50 N/cm^2 for neck muscles. Data for mammalian thigh muscles suggests a higher value of 70 N/cm2 which has been used for the study. At later stages of the work the sensitivity of this parameter will be studied. The PCSA of the muscles has been taken from Yamaguchi et al. (1990) (Appendix A).

VALIDATION OF FINITE ELEMENT MODEL WITH MUSCLES

To set up a base model, forty lower extremity muscles were added to the FE model used by Chawla et al. As a first step it was considered important to ascertain that the passive model validates against known experimental corridors. In-vivo passive response from a cadaver was modeled by setting the minimum activation level of 0.005 for each muscle and deactivating the reflex action. As the current FE model is an extension of Chawla's model, we have compared it with the simulation results reported by Chawla et al., (2004) and the experimental results of Kajzer et al., (1999).

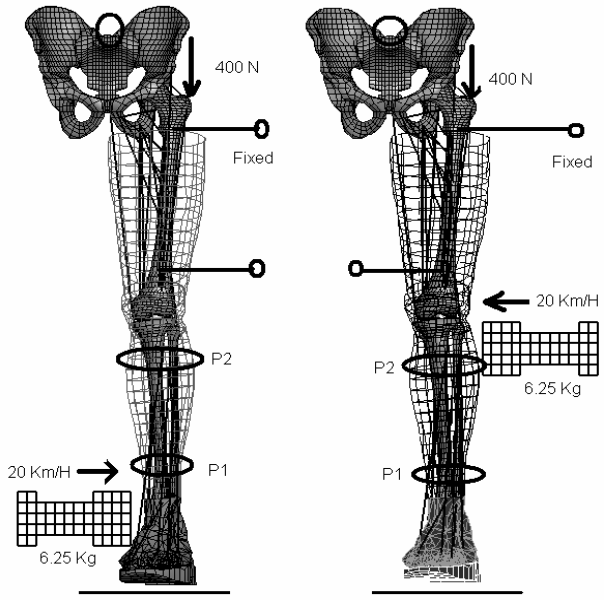

Figure 3 Simulation set up for FE model validation in bending (left) and shear (right) load at an impactor speed of 20 Km/h. Passive behavior of muscles is modeled by assigning a minimum value of 0.005 as initial activation level to each muscle.

Simulations for the validation were performed using PAM-CRASH^{TM}, an explicit dynamic solver. Figure 3 shows the set up used to perform the simulation to validate the FE model.

The sacrum and two locations of the femur were fixed (as shown in Figure 3) and a pre-load of 400 N representing body weight was applied at the top of the femur. The impactor force, lower and upper tibia displacements at locations (P1 and P2) and the ligament forces were compared with the simulation results of Chawla et al. (2004) and test results of Kajzer et al. (1999).

Comparison of passive loading cases

Figure 4 shows the impactor forces in shear loading simulations with inactivated muscles and those reported by Chawla et al., (2004) and Kajzer et al., (1999) for the impactor speed of 20 km/h. Peak impactor forces did not change significantly. Small variation in the force history is expected due to inclusion of minimum muscle forces corresponding to minimum activation levels (0.005) and the same is observed. However, the impact force correlates well with the forces reported by Chawla et al., (2004) and Kajzer et al., (1999) (correlation of 0.91 and 0.95 respectively, as obtained using the "correl" function in Microsoft Excel^{TM}).

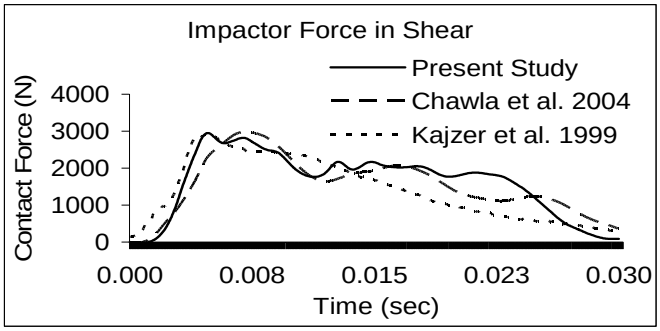

Figure 4 Comparison of Impactor force in shear loading.

Figure 5 compares the lower and upper tibia displacements (at P1 and P2 in Figure 3) for shear loading.

The lower displacements curves match with the displacement curves of Chawla et al. and Kajzer et al. shear test with correlations of 0.99 and 0.97 respectively. The upper tibial displacements show correlations of 0.99 and 0.91 respectively with respect to Chawla et al., (2004) and the experimental results respectively. The upper tibial displacements deviate slightly from the experimental results after about 15-20 ms. However, these values are very sensitive to the point chosen for recording the displacement as significant tibial rotations are observed during this phase. The current curve has been taken at a point which is just above the impactor and which was considered to be the closest to the experimental point used by Kajzer. The corresponding point has also been chosen in the Chawla et al., (2004) model for comparison.

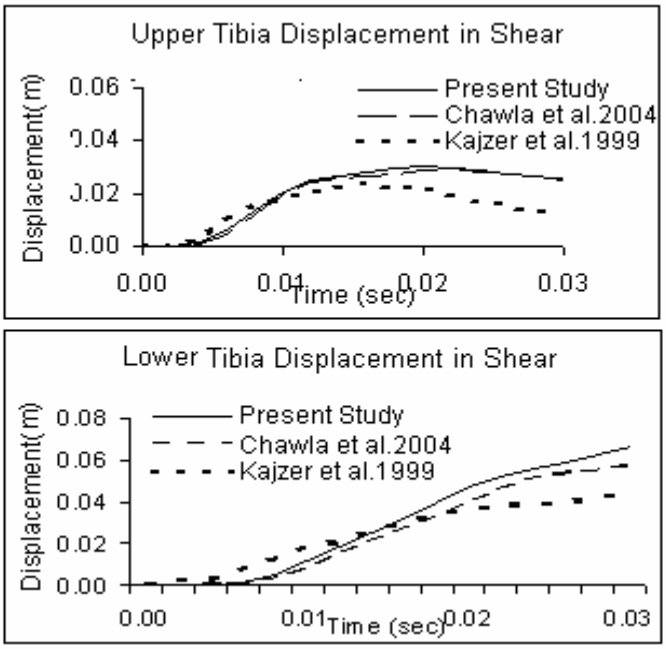

Figure 5 Comparison of upper and lower tibia displacement for 20 km/h in shear

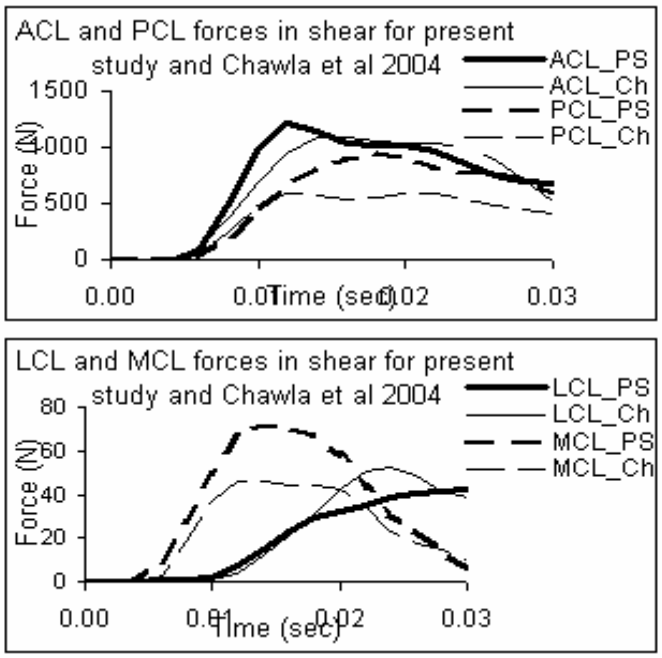

Figure 6 Comparison of forces in knee ligaments in shear load conditions for 20 km/h. (The PS curves are curves for the present study, while the Ch curves are curves from Chawla et al., 2004)

Figure 6 compares the ligament forces from the two simulations. The PCL and ACL loadings between 0.01 s and 0.03 s differ in the two simulations. In the simulations it was observed that during this period, the muscle forces were constant. However, the location of the instantaneous center of rotation (ICR) of the knee joint changes due to a change in the direction of muscle forces as shown in Figure 7. This changes the moment

arms of the muscles with respect to the effective point of knee rotation, thereby changing the torque produced by the muscles. Consequently the PCL and ACL loading were redistributed even though the external measurements like kinematics and support loading were the same.

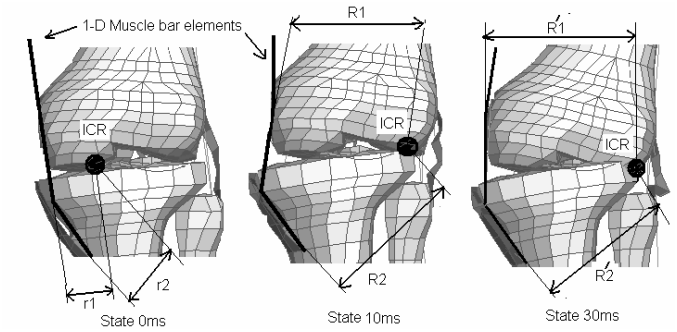

Figure 7 Change in instantaneous center of rotation and change in moment arms of muscle forces during post impact movement of the knee.

We note that the peak ligament forces in passive muscle simulations and those reported by Chawla et al., (2004) vary by about 10%. However, the experimentally measured parameters, the impactor force (corr > 0.95), and the lower extremity kinematics (corr > 0.97) match. Therefore, we conclude that the response of the FE model with minimum muscle activation captures the characteristics of cadaver knee loading. The forces in the MCL are seen to be very low. This is attributed to the ligament stiffnesses being used, which are currently as originally defined in THUMS.

SIMULATIONS FOR STANDING POSTURE

Effect of muscle activation in a free standing posture has been studied next. In these simulations, a significant difference from the Kajzer test is that the pins on the femur were not modeled. Even though the impact locations near the ankle and knee were the same, the loading did not correspond to shear and bending. They are hence referred to as below-knee and at-ankle impacts (Figure 8). There are no earlier results for free standing impact tests to compare with. To represent cadaver tests, simulations were carried out with muscle response deactivated. In the second step, the standing posture of a pedestrian with muscle activation needed to maintain stability in a gravity field is modeled using data reported by Kuo et al., (1993). Rupture of ligaments was not modeled as ligament rupture is not common in knee injuries during pedestrian accidents (Chidester and Isenberg, 2001). The response of the standing posture modeled with active muscle forces was compared with the passive model response to determine the role of muscle loading.

For simulations with deactivated muscles, the minimum muscle activation level of 0.005 was assigned to each muscle and all reflex actions were deactivated.

The activation values used to model active muscles for standing posture are listed in Table A1 in appendix A.

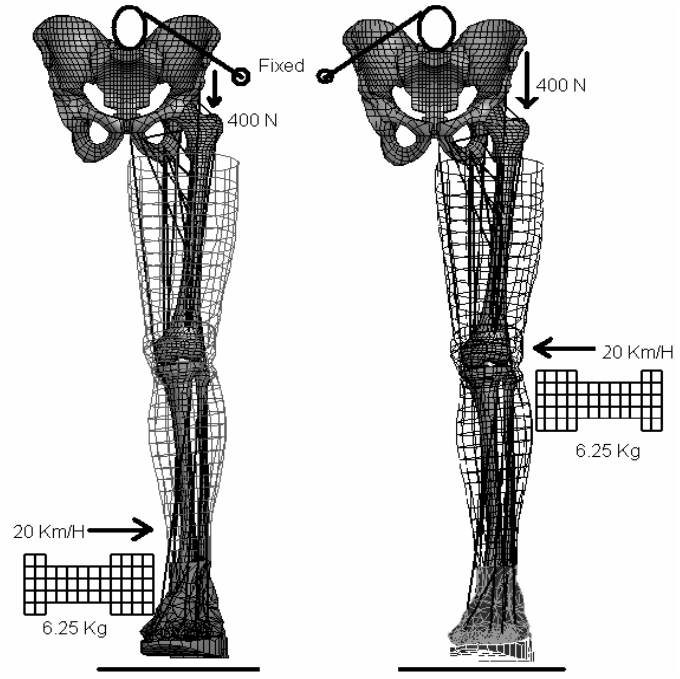

Figure 8 Simulation set up for below knee impact (left) and ankle impact (right). Constraints are removed from femur and adequate activation levels are defined in the Hill type muscle bar elements to maintain an upright standing posture.

Ackerman, (2002) has suggested a delay of 20 ms for the onset of involuntary reflex for skeletal muscles. A delay of 20 ms is therefore taken for the onset of the involuntary reflexive action after the impactor touches the leg. Stretch reflexes that automatically maintain posture were also enabled.

RESULTS AND DISCUSSION

The loading can be divided into two phases. In the initial phase, the impactor contacts the lower extremity which is initially at rest and passes energy in-elastically to the leg segments. Relative movement between tibia and femur starts only after the impactor force crosses a certain threshold, leading to fall in impactor contact forces and a shear loading in the knee joint.

In the second phase, the motion of the lower extremity creates a bending motion at the knee joint called varus and valgus. The large angular displacement between femur and tibia due to this bending motion leads to stretching in ligaments and the ligament forces peak during this phase.

BELOW-KNEE IMPACT

In simulations with activated muscles, it was observed that the impactor force reached its peak value of 2720 N about 5 ms after initial contact with the leg. During this interval no lateral movement was noticeable at the knee. As the impactor force peaks, the femur and tibia condyle

started moving laterally and away from the impactor. This event is the onset of ligament loading. In the initial phase which lasts till 10 ms, forces in the ACL, PCL and MCL increase due to shear displacement. The knee joint motion then changes from shear to valgus due to rotation of the leg. After this transition, forces in ACL and PCL decreased, whereas the force in MCL remained high till about 40 ms. A similar phenomenon was observed in simulations with deactivated muscles.

Forces in the knee ligaments for the standing posture with activated and deactivated muscles for the below-knee impact have been plotted in Figure 9. With activated muscles, a maximum force of 180 N in ACL, 60 N in PCL and 40 N in MCL was predicted. For deactivated muscles, significantly higher peak values (615N in ACL, 194N in PCL, 48 N in MCL) were predicted.

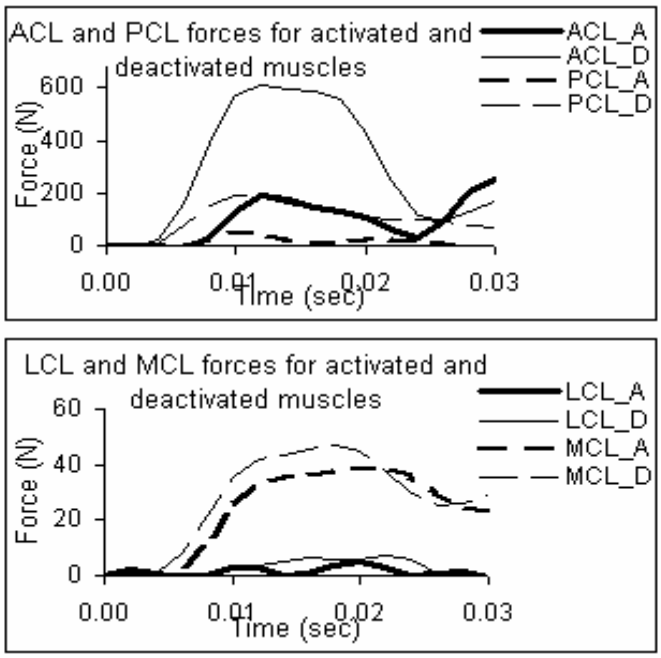

Figure 9 Comparison of forces in knee ligaments for the standing posture with below-knee impact. The A curves are curves with activated muscles and the D curves are those with deactivated muscles.

ANKLE IMPACT

Figure 10 compares forces in knee ligaments for standing posture with activated and deactivated muscles for the ankle impact.

In the simulation with activated muscles, the impactor force reaches a peak value of 2400 N in 6 ms. Over this duration no movement was noticeable in the lower leg. From 6 ms to 10 ms the lower leg forces the femur in the upward direction and a center of rotation was established at the extreme lateral point of contact between the tibia and femur condyles. Subsequently, from 10 ms to 20 ms, the lower leg continued rotating about this point. During this interval, forces in ACL and MCL increased as these ligaments along with the activated muscles resisted the tibia rotation. From 20 ms onwards, muscle forces increased due to the onset of reflex action. The foot flexed in the saggital plane away from the tibia and started rotating externally.

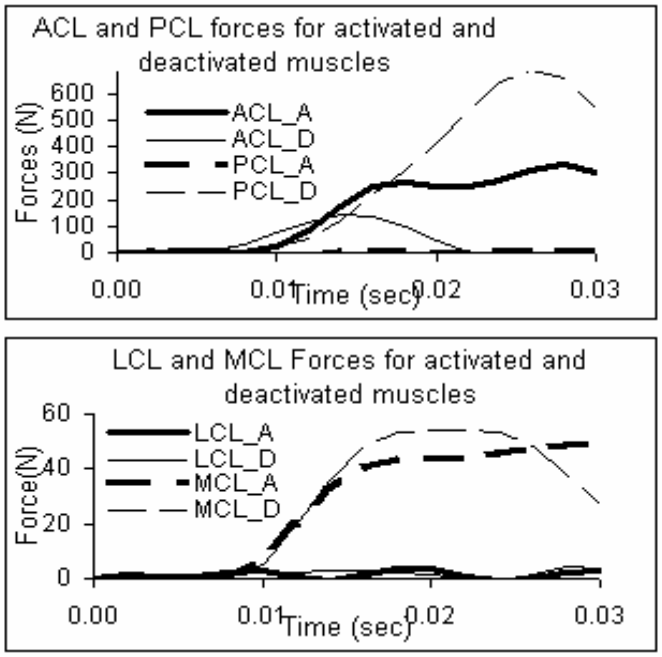

Figure 10 Comparison of forces in knee ligaments for the standing posture with ankle impact loading. The A curves are curves with activated muscles and the D curves are those with deactivated muscles.

Due to this flexion of the foot, the tibia plateau moved a little higher in the posterior side, relieving the PCL and tightening the ACL. Therefore, a second peak in the ACL force is observed (Figure 10) whereas the force in PCL has reduced.

In simulations with deactivated muscles, these events are not observed as reflex actions do not kick in. Therefore forces in PCL stay higher. Peak PCL forces for the case of deactivated muscles is about 700 N which is more than twice the peak ACL loading of 300 N in the case of activated muscles.

CONCLUSION

A lower extremity finite element model, representing a standing posture, with muscles modeled as Hill elements was developed. Reflexive muscle action was included in the model. A comparison of the shear and bending loads at low velocity lateral impacts showed a good correlation with experimental data (Kajzer et al., 1999) as well as with earlier simulation data (Chawla et al., 2004). Having thus established the suitability of the model for further study, the effect of muscle activation has then been examined in lateral impacts in the standing posture.

In lateral impacts for free standing postures, the activation of lower extremity muscles in simulation predicts a reduction in peak knee ligament forces by a factor of two or more. Since ligament loading is

predicted to be lower with muscle activation, the likelihood of ligament injury in active postures may be expected to be lower than that predicted by cadaver tests.

LIMITATIONS AND FURTHER IMPROVEMENTS

In our study, the data for point of origin and insertion was from White et al., (1989). The basis for selection of this study was the similarity in the height of the reported male specimen (177 cm) and THUMS (AM50) (175 cm), there is still a difference of 2 cm in their body height. According to Winter et al (2005) the length of the lower extremity segment is on the average 0.53 times the total body height. Using this estimate, the difference in the lower extremity segments is about 1 cm. This difference can be further reduced by using scaling techniques. Dimensions of individual segments (femur, tibia, fibula and pelvis) required to calculate scaling factors in each direction, were not available in the literature. Apart from this, THUMS represents a 50th percentile American male and its segments length are not according to the standard fraction of total body height. However, we do not anticipate that a difference of 1 cm in length of lower extremities will change the results significantly.

The effect of patella on the moment-arm seen by the quadricep muscles (vastus lateralis, vastus medialis, vastus intermediate, and rectus femoris) has not been taken into account. Thus, the torque produced by these muscles at the knee joint is underestimated. The strategy for modeling the patella effect presented by Brand et al., (1982) could be used for more accurate modeling.

In the present study we have adopted a straight line geometric model of the muscle because of the simplicity of definition using the origin and insertion locations of a muscle. This approach can lead to errors for muscles which do not work in a straight line (gracilis, semitendinosis, tibialis posterior, flexor digitorium longus, flexor hallucis longus, tibialis anterior, extensor hallucis longus, extensor digitorium longus, peroneus tertius, peroneous brevis, and peroneus longus). Multiple points could be used in the muscle definition to account for the curved path of some muscles.

For further improvements in the current finite element model, tendons should also be modeled along with the muscles to consider their effects. Other than the limitations due to muscle modeling, the basic THUMS model is not completely bio-fidelic yet as reported in Chawla et al., (2004). This could also lead to some errors.

ACKNOWLEDGEMENTS

The authors would like to acknowledge the support from the Transportation Research and Injury Prevention Program (TRIPP) at Indian Institute of Technology Delhi and the Volvo Research Foundation. The authors also acknowledge Toyota Central Research and Development Lab (TCRDL) for providing the finite element human body model, Total Human body Model for Safety (THUMS) which has been used in this study.

REFERENCES

1. Ackerman U., PDQ Physiology (2002) Ch. (2), at, www.fleshandbones.com/readingroom/pdf/226.pdf
2. Aldman, B., Kajzer, J., Bunketorp, O., Eppinger, R. (1985) An experimental study of a modified compliant bumper. In Proceedings of 10th International Technical Conference on the Experimental Safety Vehicles.
3. Ashton, S., J., Pedded, J., B., Mackay, G., M. (1977) Pedestrian injuries, the bumper and other front structure. International IRCOBI conference on the Biomechanics of Impact, pp.33-51.
4. Bhalla, K., Bose, D., Madeley, N.,J., Kerrigan, J., Crandall, J., Longhitano, D., and Takahashi, Y. (2003) Evaluation of the response of mechanical pedestrian knee joint impactors in bending and shear loading, In Proceedings of the 2003 ESV conference.
5. Bhalla, K., Takahashi, Y., Shin, J., Kam, C., Murphy, D., Drinkwater, C., J., Crandall. (2005) Experimental investigation of the response of the human lower limb to the pedestrian impact loading environment. Society of Automotive Engineers World Congress, SAE paper, 2005-01-1877
6. Bose, D., Bhalla, K., Rooij, L., Millington, S., Studley, A., and Crandall, J., (2004) Response of the knee joint to the pedestrian impact loading environment. SAE paper number 2004-01-1608.
7. Brand, R., Crowninshield, R., Wittstock, C., Pederson, D., Clark, C. and Van Frieken, F. (1982) A model of lower extremity muscular anatomy. Journal of Biomechanical Engineering 104, 304-310.
8. Brolin, K.,Halldin, P. and Leijonhfvud, I. (2005) The effect of muscle activation on neck response. Traffic injury prevention, 6: 67-76.
9. Bunketorp, O. et al., (1981) Experimental studies on leg injuries in car-pedestrian impacts. IRCOBI, pp.243-255.
10. Bunketorp, O. et al., (1983) Experimental study of a compliant bumper system. SAE Paper Number 831623.
11. Chawla, A., Mukherjee, S., Mohan, D. and Parihar, A. (2004) Validation of lower extremity model in THUMS. IRCOBI 2004.
12. Chidester, A. B., Isenberg, R. A. (2001) Final report - the pedestrian crash data study. In Proceedings of the 17 International Technical Conference on the Enhanced Safety of Vehicles.
13. Crowninshield, R. and Brand, R. A. (1981) A physiologically based criterion of muscle force prediction in locomotion. Journal of Biomechanics 14, 793-801.

14. Davy, D. T. and Audu, M. L. (1987) A dynamic optimization technique for predicting muscle forces in swing phase of gait. Journal of Biomechanics 20, 187-201.
15. Dostal, W. F. and Andrews, J. G. (1981) A three-dimensional biomechanical model of hip musculature. Journal of Biomechanics 14, 803-812.
16. Dul, J., Townsend, M., A., Shiavi, R. and Johnson, G. E. (1984 a) Muscular Synergism- I. On criteria for load sharing between synergistic muscles. Journal of Biomechanics 17, 663-673.
17. Dul, J., Johnson, G. E., Shiavi, R. and Townsend, M, A. (1984 b) Muscular Synergism- II. A minimum fatigue criteria for load sharing between synergistic muscles. Journal of Biomechanics 17, 675-684.
18. Dunmore, M., Brooks, R., McNally, D., Madeley, J., (2005). Development of an alternative frangible knee element for a pedestrian safety legform. In proceedings of 2005 IRCOBI Conference.
19. Friedrich, J. A. and Brand, R. A. (1990) Muscle fiber architecture in the human lower limb. 23, 91-95.
20. Glitch, U. and Baumann, W. (1997) The three-dimensional determination of internal loads in the lower extremity. Journal of Biomechanics 30, 1123-1131.
21. Hardt, D. E. (1978) Determining muscle forces in the leg during normal human walking –an application and evaluation of optimization methods. Journal of Biomechanical Engineering 100, 72-80.
22. Ivarsson, J., Lessley, D., Kerrigan, J., Bhalla, K., Bose, D., Crandall, J., Kent, R., (2004) Dynamic response corridors and injury thresholds of the pedestrian lower extremities. In Proceedings of 2004 IRCOBI Conference.
23. Ivarsson, J., Kerrigan, J., Lessley, D., Drinkwater, C., Kam, C., Murphy, D., Crandall, J., Kent, R. (2005) Dynamic response of corridors of the human thigh and leg in non midpoint three-point bending. Society of Automotive Engineers World Congress, SAE paper, 2005-01-0305
24. Kajzer, J., Cavallero, S., Ghanouchi, S., Bonnoit, J., (1990) Response of the knee joint in lateral impact: Effect of shearing loads. IRCOBI.
25. Kajzer, J., Cavallero, S., Bonnoit, J., Morjane, A., Ghanouchi, S., (1993) Response of the knee joint in lateral impact: Effect of bending moment. IRCOBI.
26. Kajzer, J., Schroeder, G., Ishikawa, H., Matsui, Y., Bosch, U. (1997) Shearing and Bending Effects at the Knee Joint at High Speed Lateral Loading. Society of Automotive Engineers, SAE Paper 973326.
27. Kajzer, J., Ishikawa H., Matsui Y., Schroeder G., Bosch U. (1999) Shearing and Bending Effects at the Knee Joint at Low Speed Lateral Loading. Society of Automotive Engineers, SAE Paper 1999-01-0712.
28. Kepple, T. M., Sommer, H., Siegel, K. L. and Stanhope, S. J. (1998) A three-dimensional musculoskeletal database for the lower extremities. 31, 77-80.
29. Kerrigan, J., Bhalla, K., Madeley, N., Funk, J., Bose, D., Crandall, J. (2003) Experiments for establishing pedestrian impact lower injury criteria. SAE Paper 2003-01-0895.
30. Konosu A., Issiki, T., Tanahashi M. (2005) Development of a biofidelic flexible pedestrian leg-form impactor (Flex -PLI 2004) and evaluation of its biofedility at the component level and the assembly level. Society of Automotive Engineers World Congress, SAE paper, 2005-01-1879.
31. Kuo, A. D. and Zajac, F. E. (1993) A biomechanical analysis of muscle strength as a limiting factor in standing posture. Journal of Biomechanics 26, 137-150.
32. Louie, J. K., Kuo, C. Y., Gutierrez, M. D. and Mote, C. D. J. (1984) Surface EMG measurements and torsion during snow skiing: laboratory and field tests. Journal of Biomechanics 17, 713-724.
33. Maeno, T. and Hasegawa, J. (2001) Development of a finite element model of the total human model for safety (THUMS) and application to car-pedestrian impacts. 17th international ESV conference, Paper No. 494.
34. Matsui, Y. (2001) Biofidelity of TRl legform impactor and injury tolerance of human leg in lateral impact. Stapp Car Crash Journal, Vol 45
35. Mizuno, Y. (2003) Summary of IHRA Pedestrian safety WG activities (2003) – proposed test methods to evaluate pedestrian protection afforded by passenger cars. In Proceedings of the 18th International Technical Conference on the Enhanced Safety of Vehicles.
36. Mizuno, Y. (2005) Summary of IHRA Pedestrian safety WG activities (2005) – proposed test methods to evaluate pedestrian protection afforded by passenger cars. In Proceedings of the 19th International Technical Conference on the Enhanced Safety of Vehicles.
37. Nagasaka, K., Mizuno, K., Tanaka, E., Yamamoto, S., Iwamoto, M., Miki, K. and Kajzer J. (2003) Finite element analysis of knee injury in car-to-pedestrian impacts. Traffic injury prevention, 4:345-354.
38. Pedotti, A., Krishnan, V. V. and Stark, L. (1978) Optimizing of muscle force sequencing in human locomotion. Mathl. Biosci. 38, 57-76.
39. Pierrynowski, M. R. and Morrison, J. B. (1985) A physiological model for the evaluation of muscular forces in human locomotion theoretical aspects. Mathl Biosci. 75, 69-101.
40. Pope, M. H., Johnson, R. J., Brown, D. W., and Tighe, C. (1979) The role of musculature in injuries to the medial collateral ligament. J. Bone Jt Surg. 62-A, 398-402.
41. Ramet, M., Bouquet, R., Bermond, F., Caire, Y. (1995) Shearing and Bending Human Knee Joint Tests In Quasi-Static Lateral Load. Proceeding of the International Conference on the Biomechanics of Impact (IRCOBI).
42. Schuster, J. P., Chou, C. C., Prasad, P.,Jayaraman, G. (2000) Development and validation of a

pedestrian lower limb non-linear 3-D finite element model. 2000-01-SC21, Vol. 44. Stapp Car Crash journal.
43. Seireg, A. and Arkivar, R. J. (1973) A mathematical model for evaluation of forces in lower extremities of the musculoskeletal system. Journal of Biomechanics 6, 313-326.
44. Seireg, A. and Arvikar, R.J. (1989). Biomechanical Analysis of the Musculoskeletal Structure for Medicine and Sports. Hemisphere Publishing Corporation, New York.
45. Takahashi, Y., Kikuchi, Y. (2001) Biofidelity of test devices and validity of injury criteria for evaluating knee injuries to pedestrians, Proceedings of the ESV conference.
46. Takahashi, Y., Kikuchi, Y., Mori, F., Konosu, A. (2003) Advanced FE lower limb model for pedestrians. 18th International ESV conference, Paper no. 218.
47. White, S. C., Yack, H. J. and Winters, D. A. (1989) A three dimensional musculoskeletal model for gait analysis, anatomical variability estimates. Journal of Biomechanics 22, 885-893.
48. Wickiewicz, T. L., Roy, R. R., Powell, P. L. and Edgerton, V. R. (1983) Muscle architecture of human lower limb. Clin. Ortho. Rel. Res. 179, 275-283.
49. Winters, J. M. and Stark, L. (1988) Estimated mechanical properties of synergistic muscles involoved in movements of a variety of human joints. Journal of Biomechanics 12, 1027-1041.
50. Winter D. A., (2005) Biomechanics and motor control of human movement. 3rd edition John Wiley and Sons, New Jersey.
51. World Bank (2001) Road Safety, http://www.worldbank.org/transport/roads/safety.html
52. Yamaguchi, G., Sawa, A., Moran, D., Fessler, M. and Winters, J. (1990) A survey of human musculotendon actuator parameters. In: Winters, J. Woo, S., (Eds.) Multiple Muscle Systems, Springer, New York pp. 717-773.
53. Yeo, B. P., (1976) Investigation concerning the principle of minimum total muscular force. Journal of Biomechanics 9, 413-416.

APPENDIX - A

40 lower extremity muscles are defined in the local reference frames according to White et al. (1989). Data used to define Hill muscle card for a muscle are listed in the Table A.1.

Table A.1. Data for Lower extremity muscles

Muscle	PCSA (cm^2)	L_{opt} (mm)	σ_{max}(N/cm^2)	F_{max} (N)	Na
Vastus Lateralis	17.76	336	70	1243	0.1
Vastus Intermedius	9.03	178	70	632	0.1
Vastus Medialis	14.04	294	70	982	0.1
Rectus Femoris	9.03	387	70	632	0.1
Soleus	15.08	390	70	1055	1.0
Gastrocnemius Medialis	9.88	482	70	691	1.0
Gastrocnemius Lateralis	7.73	474	70	541	1.0
Flexor Hallucis Longus	2.90	406	70	203	0.1
Flexor Digitorium Longus	1.96	424	70	137	0.1
Tibialis Posterior	3.41	391	70	238	1.0
Biceps Femoris (LH)	9.89	436	70	692	1.0
Biceps Femoris (SH)	7.24	188	70	506	1.0
Semimembranosus	9.96	409	70	697	0.1
Semitendinosus	7.99	455	70	559	0.1
Tibialis Anterior	6.28	365	70	439	0.5
Extensor Digitorium Longus	2.85	420	70	199	0.1
Extensor Hallucis Longus	2.85	230	70	199	0.1
Gracilis	5.02	427	70	351	0.1
Adductor Brevis 1	4.44	113	70	310	0.5
Adductor brevis 2	4.44	145	70	310	0.5
Adductor Longus	7.91	217	70	553	0.5
Adductor Mangus 1	8.66	97	70	606	0.5
Adductor Mangus 2	8.66	154	70	606	0.5
Adductor Mangus 3	8.66	320	70	606	0.5
Peroneus Brevis	2.97	262	70	207	1.0
Peroneus longus	4.61	381	70	322	1.0
Peroneus Tertius	1.76	140	70	123	0.1
Piriformis	8.66	105	70	606	0.1
Pectineus	7.50	104	70	525	0.1
Obturatorius Internus	9.99	68	70	699	0.1
Obturatorius Externus	3.22	72	70	225	0.1
Sartorius	4.17	525	70	291	0.1
Tensor Fasciae Latae	8.23	145	70	576	1.0
Glutaeus Maximus	16.71	160	70	1169	1.0
Glutaeus Medius 1	11.73	135	70	821	0.1
Glutaeus Medius 2	11.73	125	70	821	0.1
Glutaeus Medius 3	5.62	110	70	393	0.1
Glutaeus Minimus 1	5.62	95	70	393	0.1
Glutaeus Minimus 2	5.62	85	70	393	0.1
Glutaeus Minimus 3	5.62	80	70	393	0.1

* Na represents initial activation level in a muscle during standing posture. These values have been taken from Kuo et al., (1993).